Analyst

RSC Publishing

PAPER

A theophylline quartz crystal microbalance biosensor based on recognition of RNA aptamer and amplification of signal†

Cite this: *Analyst*, 2013, **138**, 2456

Zong-Mu Dong and Guang-Chao Zhao*

A quartz crystal microbalance (QCM) biosensor for theophylline was developed by recognition of RNA aptamer and gold nanoparticle amplification technique. Firstly, a designed small single-stranded RNA, RNA1, was immobilized onto the QCM electrode through a thiol linker. Then, the complementary stranded RNA2, which can combine with RNA1 to form a double-stranded RNA with a recognition unit of theophylline, could be self-assembled on the QCM electrode surface through a hybrid reaction in the presence of theophylline. The recognition process could cause a frequency change of QCM to give the signal related to theophylline. When RNA2 was tethered to gold nanoparticles, the signal could be amplified to further enhance the sensitivity of the designed sensor. Under the optimal conditions, the QCM-based biosensor showed excellent sensitivity (limit of detection, 8.2 nM) and specificity with a dissociation constant of $K_d = 5.26 \times 10^{-7}$ M. The sensor can be used to quantitatively detect theophylline in serum, suggesting that it can be applied in complex biological samples.

Received 29th November 2012
Accepted 14th February 2013

DOI: 10.1039/c3an36775d

www.rsc.org/analyst

Introduction

Aptamers are DNA or RNA sequences that bind specific analytes with high affinity and specificity.[1] They have several advantages over antibodies, such as simple synthesis and higher stability against pH, temperature and ionic strength.[2] Selectivity of the aptamers for the specific target is based on the systematic evolution of ligands by exponential enrichment (SELEX) process.[3,4] Typically, high affinities and specificities of aptamers toward ligands are achieved by a combination of molecular-shape complementarity, hydrogen bonding, and stacking interactions.[5] Much progress has been made in the development of aptamer-based bioanalytical assays using a variety of detection techniques such as colorimetric,[6,7] optical,[8–11] surface plasmon resonance (SPR),[12] and electrochemical analysis.[13,14] Most of the biosensing platforms require the use of labels including fluorophores and radiolabels. The labeling process introduces extra time, cost, and expertise required for the assays.

Quartz crystal microbalance (QCM) detectors have been developed to alleviate this concern. The QCM operation is often approximated by a simple principle given by the Sauerbrey equation, which enables the user to quantify directly the mass adsorbed onto the sensor surface for a given change in resonance frequency of the crystal. The methodology allows for real-time detection.

The QCM has demonstrated its effectiveness in detecting the mass of high molecular weight analytes including DNA and proteins.[15–17] However, low molecular weight analytes are difficult to detect only based on mass addition. Signal amplification could be one of the major approaches for designing and developing highly sensitive QCM-based biosensors. One successful strategy is to use the mass enhancer such as gold nanoparticles (Au NPs), which can be used in the context of an assay where free analyte is displaced with a mass-enhanced or surface-bound version of the molecule.[18,19] In the latter case, additional amplification is achieved by appending the mass tether to the linker probe.

Theophylline is used as a bronchodilator in cases of asthma, bronchitis and emphysema. Due to its toxicity, different approaches based on an aptamer for monitoring its level have been developed. Sekella and Soukup *et al.* have used fluorescence resonance energy transfer (FRET) assay for theophylline detection.[20,21] In their approach, theophylline was detected *via* monitoring the activity of a ribozyme upon theophylline binding through FRET. This is an indirect detection process. Endoh *et al.* designed a theophylline–aptamer-inserted RNA to detect theophylline with a limit of detection less than 10 μM by FRET.[22] Moreover, electrochemical,[23–26] optical[27] and fluorescent[5] methods for the detection of theophylline have also been reported by use of an RNA aptamer, which was subsequently improved to detect theophylline in serum.[28,29] However, these methods involve long analysis time and the use of fluorescent and redox-active labels.

Anhui key laboratory of Chem-Biosensing, School of Chemistry and Materials Science, Anhui Normal University, Wuhu, 241000, P. R. China. E-mail: gczhao@mail.ahnu.edu.cn; Fax: +86-553-5910720; Tel: +86-553-5910721

† Electronic supplementary information (ESI) available. See DOI: 10.1039/c3an36775d

In this work, we have fabricated a highly sensitive QCM-based biosensor for simple and rapid theophylline detection using Au NPs to enhance frequency signals. QCM is a useful analytical method to assess sensor surface layer phenomena, such as self-assembled monolayer and analyte capture. Moreover, according to previous studies, the two RNA aptamers, 11-mer and 8-mer theophylline binding aptamer (RNA1 and RNA2), can bind to each other to form a special recognition unit for theophylline,[22,30] which has facilitated the successful fabrication of a sensing system to analyze theophylline. The methodology is simple, allows real-time detection, and does not require the use of harmful reagents, such as radio-labeled ligands or expensive chromophoric substrates. Remarkably, the theophylline standard spiked serum sample was also used for exploring the potential of this method in practical applications.

Experimental

Materials and chemicals

Oligonucleotides tethered with a thiol linker were purchased from Integrated DNA Technologies and used without further purification. The designed sequence is HS–$(CH_2)_6$–5′-CCU-UGG AAG CC-3′ (RNA1), which was used as the capturing probe sequence. Its complementary sequence is 5′-GG AUA CCA-3′–$(CH_2)_6$–HS (RNA2), which can bind to the capturing probe to form a special recognition unit for theophylline. Tris (2-carboxyethyl) phosphine hydrochloride (TCEP) was used as the reducing agent to reduce the disulfide bonds formed in the synthesized procedure of HS–ssRNA. $HAuCl_4 \cdot 4H_2O$ was purchased from Shanghai Chemical Reagents (Shanghai, China). All other chemicals were of analytical grade and used without further purification.

Apparatus

QCM was performed on a quartz crystal microbalance (CHI 440A, Shanghai Chenhua Ltd. China). A 7.995 MHz AT-cut quartz crystal (13.7 mm diameter) covered with gold electrodes ($\varnothing = 5$ mm) was mounted levelly in a homemade Taflon holder. This Taflon holder was linked with a six-channel BT100K peristaltic pump. Electrochemical impedance spectroscopy (EIS) and cyclic voltammetry (CV) were carried out with an electrochemical workstation (CHI660C, Shanghai Chenhua Ltd., China). CV and EIS were performed in 5 mM $[Fe(CN)_6]^{3-/4-}$ solution which was purged with highly purified nitrogen for at least 15 min. The prepared modified electrode was used as the working electrode. An Ag/AgCl electrode and Pt wire were used as the reference electrode and the auxiliary electrode, respectively. All the measurements were carried out at room temperature.

Synthesis and functionalization of gold nanoparticles

Au NPs were prepared according to a previously reported method with a minor modification.[31] In brief, 5 mL of trisodium citrate (1%) was added to 100 mL of boiling $HAuCl_4$ solution (0.25 mM) under stirring for 10 min. The resulting solution was allowed to cool to room temperature. The size of Au NPs obtained was evaluated by using a JEM-100CX transmission electron microscope (JEOL, Tokyo, Japan, figure not shown).[32] The prepared Au NPs, with an average size of 13 nm, were used for binding with RNA2. The concentration of the prepared Au NPs was 0.15 μM, determined by a U-3010 UV-vis spectrophotometer (Hitachi, Tokyo, Japan) with the absorbance at 520 nm and the molar extinction coefficient is $2.7 \times 10^8\ M^{-1}\ cm^{-1}$. The as-prepared Au NPs were further co-modified with the RNA2, which was denoted as RNA2–AuNPs. Briefly, Au NPs (5 mL, 25 nM) were incubated with a RNA2 probe solution (100 μL, 100 μM) for 12 h at room temperature. The final mixture was slowly brought up to a final salt concentration of 0.1 M NaCl, 10 mM TCEP and 10 mM PBS (pH 7.4) and allowed to age for 24 h. Centrifugation was performed at 14 000 rpm for 40 min in order to remove excess RNA2. The precipitate was washed with 0.1 M NaCl, 10 mM PBS (pH 7.4) solution, recentrifuged, and finally dispersed in 10 mM PBS (pH 7.4) containing 0.1 M NaCl for further use. The supernatant solution was used to determine the excess RNA2 by spectrophotometric method. The surface density of RNA2 on the Au NP could be determined. In brief, with standard stock solutions containing different concentrations of RNA2, the absorbance was determined at 260 nm. Then, the standard curves were obtained. The absorbance of the supernatant solution was also determined simultaneously, and the excess RNA2 could be detected. The surface density of RNA2 on the Au NPs could be calculated *via* the D-value of RNA2 concentration before and after incubating with Au NPs.

Direct immobilization of the RNA1 aptamer on QCM electrode

The RNA1-modified QCM electrode was prepared according to the literature with some modification.[18] Briefly, the QCM gold electrodes were cleaned with Phiranha solution [H_2O_2–H_2SO_4 1 : 3 (v/v)] for 1 min, rinsed with copious amounts of purified water and ethanol, and dried with a gentle flow of nitrogen in order to remove pollutants from the electrode surface. Prior to the immobilization of the electrodes, RNA1 stock solution (0.1 mM) was reduced in 10 mM TCEP for 2 h to cleave disulfide bonds. The resulting solution was then diluted with Tris–HCl buffer (pH 7.4) to a desired concentration (50 μM). Then, the QCM electrode was incubated in the RNA1 solution for 16 h in the dark at 4 °C. Followed by incubation, the electrode was rinsed with water and then immersed in an aqueous solution of 1 mM 6-mercapto-1-hexanol for 1 h to block the uncovered electrode surface.[33] As a final step, the electrode was rinsed with water, dried with nitrogen, and stored at 4 °C prior to use. The assembly procedure of the electrode was shown in Scheme 1.

QCM measurements

All QCM experiments were performed in a QCM cell, in which the quartz crystal gold electrodes were modified with the capturing probe. The experimental process could be described as follows: 10 mM Tris–HCl buffer (pH 7.4) containing 0.1 M NaCl was injected firstly into the QCM cell with a flow rate of 20 $\mu L \cdot min^{-1}$, and the crystal frequency was measured as a background signal. After the signal change was less than 1 Hz of frequency drift in 60 s, the experiment could be continued.

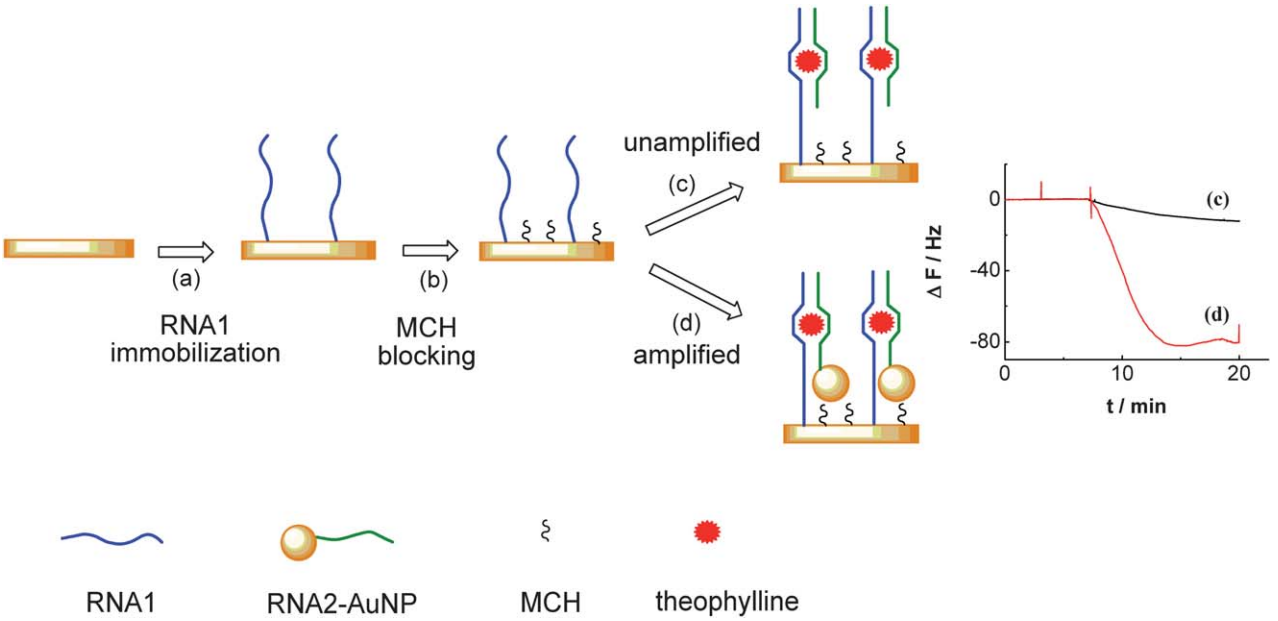

Scheme 1 Schematic diagram illustrating the surface preparation (a and b) and binding procedure of the sensing interface for detection of theophylline based on RNA2 (c) and RNA2–AuNPs conjugates (d).

Then, 50 μM linking probe (RNA2 or RNA2–(AuNPs)) solution was added at a flow rate of 20 $\mu L \cdot min^{-1}$ and the signal (ΔF) of the QCM-based sensor was recorded. Then, the standard solution of theophylline was injected into the QCM cell by using a micro-injector and the solution in the QCM cell was kept still until a stable signal (ΔF) was obtained. Control experiments were performed in a similar fashion but without adding the theophylline.

Analysis of standard spiked serum samples

Initially, 0.5, 2.0 and 5.0 mL fetal calf serum (Hyclone Laboratories, Logan, UT, USA) were spiked with theophylline standard. The mixtures were diluted to 20 mL by Tris–HCl buffer to make a final theophylline concentration of 0.1 μM. Shaken for 10 min and centrifuged for 20 min at 14 000 rpm, the supernatants were separated from the solution for theophylline determination.

Results and discussion

The design of the sensing system

The sensing strategy in this study involved the self-assembly of the thiolated aptamer (RNA1), recognition of theophylline through forming a complex composed of RNA1, RNA2 and theophylline, and signal amplification with gold nanopaticles. Scheme 1 shows the procedure of the amplified sensing of the target molecule. Firstly, RNA1 was immobilized on a QCM electrode to form an aptamer monolayer, which was used as a capturing chip and set in buffer solution. When only RNA2–AuNPs was injected to the solution, the frequency signal of QCM remained almost unchanged. However, when the mixture solution of theophylline (0.45 μM) and RNA2–AuNPs was injected, the frequency signal of QCM decreased 87 Hz within 10 min due to forming a recognition complex of RNA1/theophylline/RNA2–AuNPs (procedure d of Scheme 1). The QCM sensor responds for theophylline more quickly (10 min) compared to most QCM sensor response times for other targets,[33–35] and has a similar response time compared to IP_{20}-immobilized QCM biosensor for protein kinase detection.[17] The availability of the above complex is based on the fact that RNA1 and RNA2 can recognize two distinct sites on theophylline.[22,30] Such binding events typically involve ligand-induced structural changes in the aptamers, resulting in the formation of unique secondary structures responsible for ligand binding, in which the internal-loop structures are representative of active sites for binding events.[5] As a control experiment, the mixture solution of individual RNA2 and theophylline was injected in the biosensor, the response of the biosensor was also observed (procedure c of Scheme 1). However, the signal response of biosensor was far below that of the procedure b (use of RNA2–AuNPs) under the same concentration of theophylline. In this study, Au NPs were used as signal enhancers for highly sensitive detection of theophylline. Compared with sensors prepared without a signal amplifier (Au NPs), the biosensor displayed an increase of about two orders of magnitude in the detection limit.

Electrochemical characterizations of sensing interface

Cyclic voltammetry (CV) and electrochemical impedance spectroscopy (EIS) were utilized to characterize the steps of electrode modification and sensing of theophylline. At the bare gold electrode, a couple of well redox peaks of $[Fe(CN)_6]^{4-/3-}$ could be observed, as shown in Fig. 1A (curve a). Then, the gold electrode was incubated in a RNA1 solution for 16 h. Following the incubation, the electrode was washed with water and

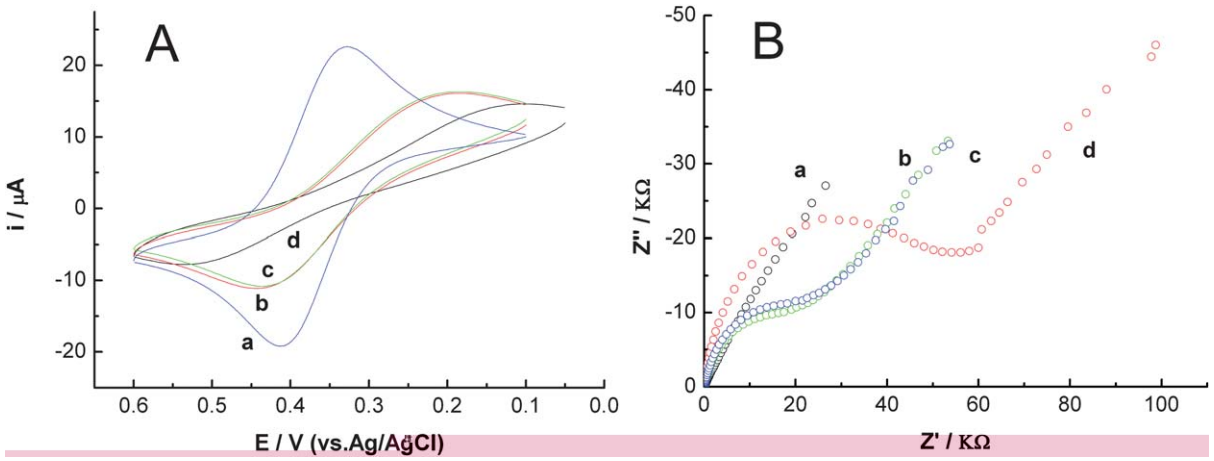

Fig. 1 Characterization of the sensing interface by CV and EIS. (a) bare electrode, (b) after immobilization of RNA1 probe, (c) incubation with 1 μM RNA2–AuNPs solution without theophylline for 30 min, (d) incubation with 1 μM RNA2–AuNPs solution containing 0.05 μM theophylline for 10 min.

immersed in an aqueous solution of 1 mM 6-mercapto-1-hexanol for 1 h to remove non-specifically adsorbed aptamer molecules and block the electrode surface. Subsequently, the gold electrode immobilized with RNA1 and 6-mercapto-1-hexanol was used as a work electrode and CV was performed in the same $[Fe(CN)_6]^{4-/3-}$ solution. As shown in Fig. 1A (curve b), the peak currents obviously decreased (more than 8 μA) and the difference between cathodic and anodic peak potential increased. These results suggest the formation of a dense monolayer of immobilized RNA1 and 6-mercapto-1-hexanol on the gold electrode surface. The RNA1 and 6-mercapto-1-hexanol on the electrode surface prohibited the electron transfer of $[Fe(CN)_6]^{4-/3-}$ at the electrode interface. Following this step, the electrode was immersed in 1 μM RNA2–AuNPs solution (containing 10 mM PBS and 0.1 M NaCl) for 30 min. The obtained CV response, Fig. 1A (curve c), was very similar to Fig. 1A (curve b), revealing that the electrode surface did not change obviously. However, when the electrode was immersed into RNA2–AuNPs solution containing 0.05 μM theophylline for 10 min, hardly any of the redox peaks of $[Fe(CN)_6]^{4-/3-}$ could be observed, as shown in Fig. 1A (curve d). This was likely to be attributed to the formation of the structure of RNA1/theophylline/RNA2–AuNPs, which further blocked the electron transfer of $[Fe(CN)_6]^{4-/3-}$ at the electrode surface. These results could also be demonstrated by EIS, which was shown in Fig. 1B. As the electrochemical impedance was related to the amount of theophylline, thus it could also be measured by EIS. However, the reproducibility and sensitivity of this method were not as good as those of QCM, so the latter was utilized to detect theophylline in our work.

Sensitivity of aptamer–AuNPs amplified QCM biosensor

Sensitivity and specificity of aptamer–AuNPs amplified QCM biosensor are dependent upon aptamer affinity, orientation, and sensor surface coverage. In this study, the RNA1 were immobilized onto a gold QCM surface. Samples containing different theophylline concentrations were sequentially added to the QCM sensor to produce the calibration curve. The amount of RNA1 on the chip surface was kept high to ensure that aptamer binding sites would not become saturated upon the sequential addition of theophylline. The surface coverage of RNA1 on the sensor surface was detected by QCM. When the density reached about 6.52×10^{14} molecules cm^{-2}, the response signal arrived at the maximum, which could be ascribed to the saturation of immobilized RNA1 probe molecules on the sensor surface (the surface coverage was calculated on the basis of the ΔF measured during the QCM experiments).[36] The surface coverage of RNA1 probe molecules on the sensor surface was also calculated to be 8.75×10^{13} molecules cm^{-2} by Tarlov's electrochemical method.[37] This value is less than 6.52×10^{14} molecules cm^{-2} by the QCM method. The surface coverage of the RNA1 probe calculated by QCM may also contain the contributions from the thimbleful of coupled water on the sensor surface.

Amplification effect of Au NPs was studied subsequently by using an RNA1-modified QCM chip. Firstly, the direct detection of theophylline was studied through monitoring the QCM responses induced from theophylline binding with immobilized RNA1 by the formation of RNA1/theophylline/RNA2 on the QCM biosensor surface. As shown in Fig. 2b, with the increase of theophylline concentrations from 0.45 to 1.5 μM, the frequency shifts from −5.5 to −18 Hz were observed. For theophylline concentrations lower than 0.12 μM, it is difficult to discriminate the frequency response from the baseline noise. When RNA2 was replaced by RNA2–AuNPs in the experimental process, the frequency shift obviously increased with the same concentration of theophylline (frequency shifts from −95 to −215 Hz were observed), as shown in Fig. 2c. This could be explained by the fact that Au NPs were introduced as a signal enhanced reagent to further improve the sensitivity of the detector. A control experiment (monitor QCM signal over time without addition of RNA2 or RNA2–AuNPs) was shown in Fig. 2a, which revealed that sensor drift over time was minimal and did not impact on the measurements.

adenine are similar to theophylline. A solution of standard sample of adenine (2.5 μL, 2 mM), guanine (2.5 μL, 2 mM) or caffeine (4 μL, 2 mM) was added in 1 mL PBS solution in the QCM chamber, respectively. Fig. 5 shows the response of the designed biosensor to the three control reagents. The adsorption detection was small when caffeine (8 μM), guanine (5 μM) and adenine (5 μM) were added to the aptamer–AuNPs amplified QCM biosensor. Less than 2 Hz signal shifts (curve 1 to curve 3) were observed implying non-significant binding activity of the present aptamer–AuNPs amplified QCM biosensor for caffeine, guanine and adenine (compared to a 122 Hz decrease when the solution containing 0.8 μM of theophylline was added to the same system). The data were summarized as Fig. S2 and displayed in the ESI.† In order to evaluate the binding affinity between theophylline and aptamers, the theophylline–aptamer association constant (K_a) can be obtained from the time relationship of frequency decrease at various theophylline concentrations. Based on a Langmuir adsorption isotherm,[39] the association (K_a) and dissociation (K_d) constants for theophylline–aptamer binding can be described by eqn (1).

$$\frac{C_{THE}}{\Delta M} = \frac{C_{THE}}{\Delta M_{max}} + \frac{1}{\Delta M_{max} K_a} \quad (1)$$

In eqn (1), ΔM_{max} is the maximum amount that theophylline can be bound on the biosensor surface, which is equivalent to the binding of theophylline when all the RNA1 are converted to the RNA1/theophylline/RNA2–AuNPs complex. ΔM is the measured theophylline binding amount at equilibrium, which is a function of the theophylline concentration and will not change with time, and $[C_{THE}]$ is the original concentration of theophylline. Based on the data obtained from Fig. 4, we can obtain a representative plot of $[C_{THE}]/\Delta M$ *versus* $[C_{THE}]$ (Fig. 6). According to eqn (1), the association constant (K_a) can be obtained by the ratio of slope to the intercept of the calibration curve. The dissociation constant (K_d) can be calculated as 5.26×10^{-710}

Table 1 Results obtained in analysis of diluted serum samples with the QCM-based sensor ($n = 5$)[a]

Serum sample dilution folds	Concentration (nM)								
	Added	Found					Avg. found	RSD%	Recovery%
5	100.0	119.5	113.7	98.8	123.6	111.6	113.6	9.4	113.6
10	100.0	107.4	109.9	112.6	119.6	99.5	109.8	7.3	109.8
15	100.0	98.8	106.6	99.2	110.5	103.5	103.7	5.0	103.7

[a] No theophylline was detected in diluted original serum samples.

Conclusions

In this work, the special sequence of RNA aptamers with the recognition unit of theophylline were designed, and an aptamer-based QCM biosensor was developed for the sensitive detection of theophylline. The amplification effect of Au NPs on QCM as the mass enhancers was demonstrated in the analytical method. With the amplification, a low detection limit of 8.2 nM was achieved. The spiked recovery of theophylline from fetal calf serum is satisfactory. This work extends the application of QCM in biosensors, and provides a promising approach for the sensitive detection of bio-reagents in biological samples.

Acknowledgements

This work was supported by the National Natural Science Foundation of China (20975001), the Educational Administration of Anhui Province (kj2010b354) and the Innovation Funds of Anhui Normal University (2010cxji16).

Notes and references

1 S. D. Jayasena, *Clin. Chem.*, 1999, **45**, 1628.
2 L. C. Jorge, L. Wanda, K. L. Nancy and O. S. Morley, *Biosens. Bioelectron.*, 2010, **26**, 23.
3 A. D. Ellington and J. W. Szostack, *Nature*, 1990, **346**, 818.
4 C. Tuerk and L. Gold, *Science*, 1990, **249**, 505.
5 M. J. Li, Y. Sato, S. Nishizawa, T. Seino, K. Nakamura and N. Teramae, *J. Am. Chem. Soc.*, 2009, **131**, 2448.
6 J. S. Lee, A. U. Pirmin, M. S. Han and C. A. Mirkin, *Nano Lett.*, 2008, **8**, 529.
7 J. Liu and Y. Lu, *Anal. Chem.*, 2004, **76**, 1627.
8 N. Li and C. M. Ho, *J. Am. Chem. Soc.*, 2008, **130**, 2380.
9 C. Teller, S. Shimron and I. Willner, *Anal. Chem.*, 2009, **81**, 9114.
10 F. Pu, Z. Z. Huang, J. S. Ren and X. G. Qu, *Anal. Chem.*, 2010, **82**, 8211.
11 N. Tuleuova, C. N. Jones, J. Yan, E. Ramanculov, Y. Yokobayashi and A. Revzin, *Anal. Chem.*, 2010, **82**, 1851.
12 J. L. Wang and H. S. Zhou, *Anal. Chem.*, 2008, **80**, 7174.
13 M. Y. Ho, N. D. Souza and P. Migliorato, *Anal. Chem.*, 2012, **84**, 4245.
14 Y. L. Wen, H. Pei, Y. Wan, Y. Su, Q. Huang, S. P. Song and C. H. Fan, *Anal. Chem.*, 2011, **83**, 7418.
15 F. Patolsky, A. Lichtenstein and I. Willner, *J. Am. Chem. Soc.*, 2000, **122**, 418.
16 S. M. Knudsen, J. Lee, A. D. Ellington and C. A. Savran, *J. Am. Chem. Soc.*, 2006, **128**, 15936.
17 X. H. Xu, J. Zhou, X. Liu, Z. Nie, M. Qing, M. L. Guo and S. Z. Yao, *Anal. Chem.*, 2012, **84**, 4746.
18 J. S. Mitchell, Y. Wu, C. J. Cook and L. Main, *Anal. Biochem.*, 2005, **343**, 125.
19 Z. M. Dong and G. C. Zhao, *Sensors*, 2012, **12**, 7080.
20 P. T. Sekella, D. Rueda and N. G. Walter, *RNA*, 2002, **8**, 1242.
21 G. A. Soukup and R. R. Breaker, *Proc. Natl. Acad. Sci. U. S. A.*, 1999, **96**, 3584.
22 T. Endoh, R. Shintani, M. Mie, E. Kobatake, T. Ohtsuki and M. Sisido, *Bioconjugate Chem.*, 2009, **20**, 2242.
23 G. C. Zhao and X. Yang, *Electrochem. Commun.*, 2010, **12**, 300.
24 S. Riahi, M. F. Mousavi, S. Z. Bathaie and M. Shamsipur, *Anal. Chim. Acta*, 2005, **548**, 192.
25 A. Kotani, M. Hashimoto, T. Kotani and F. Kusu, *J. Electroanal. Chem.*, 2011, **656**, 85.
26 E. E. Ferapontova, S. Shipovskov and L. Gorton, *Biosens. Bioelectron.*, 2007, **22**, 2508.
27 L. C. Jorge, L. Wanda, K. L. Nancy and O. S. Morley, *Biosens. Bioelectron.*, 2010, **26**, 23.
28 E. E. Ferapontova, E. M. Olsen and K. V. Gothelf, *J. Am. Chem. Soc.*, 2008, **130**, 4256.
29 E. E. Ferapontova and K. V. Gothelf, *Langmuir*, 2009, **25**, 4279.
30 R. D. Jenison, S. C. Gill, A. Pardi and B. Polisky, *Science*, 1994, **263**, 1425.
31 J. Q. Zhang, Y. S. Wang, Y. He, T. Jiang, H. M. Yang, X. Tan, R. H. Kang, Y. K. Yuan and L. F. Shi, *Anal. Biochem.*, 2010, **397**, 212.
32 X. M. Li, P. Y. Fu, J. M. Liu and S. S. Zhang, *Anal. Chim. Acta*, 2010, **673**, 133.
33 J. Wu, D. M. Cropek, A. C. West and S. Banta, *Anal. Chem.*, 2010, **82**, 8235.
34 Z. Shen, M. Huang, C. Xiao, Y. Zhang, X. Zeng and P. G. Wang, *Anal. Chem.*, 2007, **79**, 2312.
35 W. A. Henne, D. D. Doorneweerd, J. Lee, P. S. Low and C. Savran, *Anal. Chem.*, 2006, **78**, 4880.
36 A. Kira, H. Kim and K. Yasuda, *Langmuir*, 2009, **25**, 1285.
37 A. B. Steel, T. M. Herne and M. J. Tarlov, *Anal. Chem.*, 1998, **70**, 4670.
38 R. B. Pernites, R. R. Ponnapati and R. C. Advincula, *Macromolecules*, 2010, **43**, 9724.
39 Z. H. Shen, H. P. Yan, F. F. Parl, R. L. Mernaugh and X. Q. Zeng, *Anal. Chem.*, 2007, **79**, 1283.
40 J. Zhang, S. Song, L. Zhang, L. Wang, H. Wu, D. Pan and C. Fan, *J. Am. Chem. Soc.*, 2006, **128**, 8575.

